Phasic Ion Channel Blockade

A Kinetic Model and Parameter Estimation Procedure

C. Frank Starmer and Augustus O. Grant

Departments of Medicine and Computer Science, Duke University Medical Center, Durham, North Carolina 27710

SUMMARY

For excitable membranes, use and frequency dependence represent a progressive incorporation of drug into gated ion channels with repetitive stimulation. In contrast to receptors where access to ligand is continuous in time, we define guarded receptors, such as gated ion channels, as receptors whose access to the ligand pool is transient and controlled by the channel-gating process. During repetitive stimulation, the fraction of ligand-bound channels (ion channel blockade) follows an exponential time course, determined by the interstimulus interval, channel-gating processes, drug concentration, and the forward and reverse rate coefficients characteristic of the binding process. Based on a first order model of ligand-receptor binding, we derive a characterization of ion channel blockade via a single diffusion path under conditions of repetitive phasic stimulation. Extension to multiple diffusion paths and multiple drugs leads to a more complex scheme, but these generalizations are straightforward. For the case of one diffusion path, we derive the steady state level of channel blockade for guarded receptors as a function of stimulus rate and develop a data analysis strategy suitable for characterizing ion channel-blocking agents such as local anesthetics and antiarrhythmic drugs. We show that as receptor access time increases, the transient and steady state properties of guarded receptors become equivalent to those derived from the standard continuous access ligand-receptor model. The analysis tools presented simplify the quantitative description of the functional properties of many ion channel blockers and appear to have general applicability to characterization of periodically accessible receptors.

INTRODUCTION

Recently (1) we proposed a simplification of the modulated receptor hypothesis of ion channel blockade. Termed the guarded receptor hypothesis, we considered simple first order blockade of channel-blocking agents with a sodium channel-binding site of fixed affinity. In contrast to the modulated receptor hypothesis (2, 3), we found it unnecessary to postulate modified channel gate kinetics in drug-complexed channels. We viewed migration of drug between drug pools and the binding site as controlled by the channel-gating apparatus. We postulated a guarding effect where closed conformation gates inhibit drug ingress to the interior binding site. In addition, we postulated a trapping effect where closed conformation gates inhibit unbinding by trapping drug within the channel. The resulting model accounted for observed shifts in apparent channel inactivation (4) and apparent shifts in receptor affinity (5), as well as use and frequency dependence (4, 6–8).

Conspicuously absent from our original communication was a method for estimating the kinetic parameters governing drug-channel interactions. The time-varying nature of receptor access prevented a closed form solution of the differential equation describing blockade. However, recent single channel measurements (9, 10) suggest a major simplification of the original computational model. In particular, many channels appear to open once during a depolarizing pulse and remain open for only a short time. It seems reasonable to partition the temporal cycle of a periodically excited cell into regions of homogeneous conditions while ignoring the transitions between phases of the cycle and also ignoring the random variation in state transition times. Thus, we have assumed all binding sites in a membrane patch become simultaneously accessible and remain accessible for an interval equal to the mean receptor access time. We further have assumed the interval between the end of the accessible interval and the end of the depolarizing pulse is negligible compared with the recovery interval. With these assumptions, it is feasible to derive an equation for channel blockade similar to that used to describe binding of a ligand to a continuously accessible receptor.

In this communication, we present a new model and an associated procedure for estimating kinetic binding parameters from data derived from pulse train stimulation. The model provides a theoretical basis for three observed effects: 1) exponential relationships between acquired blockade and time; 2) linear relationships between uptake rate, stimulus interval, and drug concentration; and 3) a linear relationship between steady state blockade and the state-dependent equilibria. The analysis tools derived herein parallel those for estimating kinetic parameters of continuously accessible receptors. The method is a general procedure that can be adjusted for the particular combination of drug(s), access path(s), and gating effects under investigation. Analyses of several published studies suggest the method can aid in quantitatively characterizing ion channel-blocking agents.

EXPERIMENTAL PROCEDURES

Methods. With pulse train stimulation, we assume that during shifts of the membrane potential, channel-binding sites switch between guarded (inaccessible) and unguarded (accessible) status. Similarly, in drug-complexed channels, the bound receptors switch between trapped and untrapped status. Based on a first order binding process, the fraction of blocked channels will follow an exponential time course with a time constant determined by the binding and unbinding rates, drug concentration, receptor accessibility, and stimulus intervals. When the stimulus interval is less than four recovery time constants, the fraction of blocked channels accumulates from one stimulus pulse to the next. This accumulated block is referred to as use- or frequency-dependent block. As new theoretical results, we show that the envelope of the net blockade developed during pulse train stimulation (the curve connecting peak-measured blockade at each stimulus pulse) follows an exponential time course determined by the kinetic rate constants, stimulus rates, drug concentrations, and the unguarded and untrapped intervals. Furthermore, we show that the rate of development of use-dependent blockade is a linear combination of the rates associated with the depolarizing and repolarizing intervals of the stimulus and that steady state block is linearly related to an exponential function of the uptake rate.

To develop the analytical description of pulse train-induced blockade, we note that blockade during the current stimulus interval can be mathematically related to blockade in the previous interval. To illustrate, we divide each stimulus period into intervals of constant conditions. For the simplest case of a single gated channel, consider a stimulus interval as having two subintervals of duration, t_d and t_r, as shown in Fig. 1. During the depolarization interval, t_d, a fraction f_d of the unblocked channels has a low impedance diffusion path between drug pool and channel-binding site (unguarded access), while for a fraction g_d of blocked channels, drug is not trapped within the channel (1, 11) and is thus free to unbind, resulting in a blockade time constant τ_d. During the recovery time, t_r, a fraction f_r of the unblocked channels is accessible and a fraction g_r of the blocked channels is untrapped, resulting in a time constant τ_r.

The resulting process for a single stimulus period (depolarizing interval followed by a repolarizing interval) is considered as two sequential processes described by

$$\text{depolarizing phase: } D + U \underset{g_d l}{\overset{f_d k}{\rightleftharpoons}} B$$

$$\text{repolarizing phase: } D + U \underset{g_r l}{\overset{f_r k}{\rightleftharpoons}} B$$

During each phase of the stimulus, the time course of blockade, b, is characterized by the solution of

$$\frac{db}{dt} = fk[D](1 - b) - glb \quad (1)$$

For f and g constant during an interval,

$$b(t) = b(\infty) + (b(0) - b(\infty))e^{-t/\tau} \quad (2)$$

$$= b(0)e^{-t/\tau} + b(\infty)(1 - e^{-t/\tau}) \quad (3)$$

where $b(0)$ is the initial block, $b(\infty)$ is the equilibrium block, and τ is the time constant of blockade. The equilibrium block, $b(\infty)$, and τ, the time constant of blockade associated with each interval of the stimulus protocol, are defined by

$$b(\infty) = \left(1 + \frac{gl}{fk[D]}\right)^{-1} \quad (4)$$

$$\tau = (fk[D] + gl)^{-1} \quad (5)$$

where f and g are defined by the channel-gating model and may be voltage sensitive. With repeated stimulation, the channel is subjected to various blocking and unblocking processes. As the next interval occurs, the block derived during the prior interval becomes an initial condition for the next blockade process. The resulting sequence of blockade equations characterizes block acquired during each phase of the stimulus protocol and can be described as a recurrence relationship, i.e., blockade for the nth stimulus is defined in terms of blockade acquired during the n–1th stimulus. These recurrence equations have a direct solution.

Blockade defined as a recurrence relation. Here we derive an expression for the fraction of blocked channels for a two-phase protocol (Fig. 2). The two-phase protocol consists of switching the stimulus voltage between a depolarizing potential and a repolarizing potential. During each phase, channel gates change conformation, thereby introducing variation in the fractions of guarded unblocked channels and trapped blocked channels. We assume that during the depolarizing phase, the channels switch to an open conformation for a short time, followed by a closed period for the remainder of the depolarizing interval.

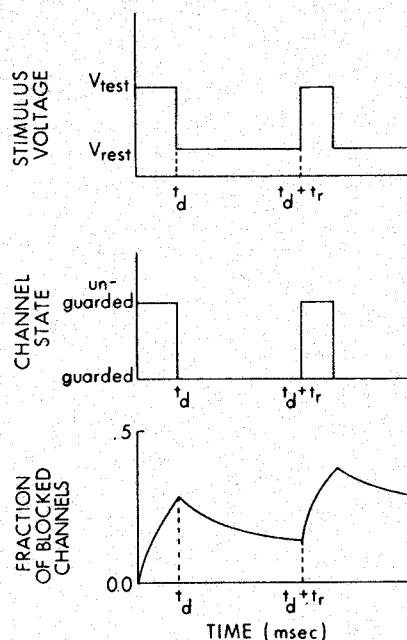FIG. 1. *Idealized relationships between stimulus, channel state transitions, and the fraction of blocked channels*

During a depolarizing test potential, the channels change from closed to open conformations, thus allowing drug to diffuse to the channel interior binding site. During the recovery period when the membrane potential is at a resting level, drug-complexed channels can become unbound and diffuse out of channels.
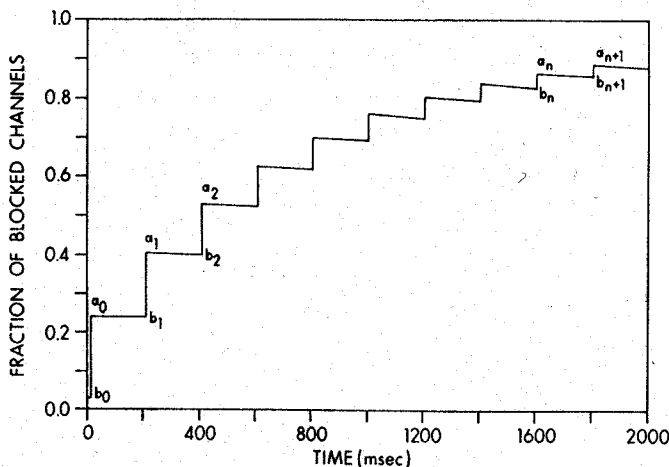
FIG. 2. *The time course of acquired blockade during repetitive stimulation*

During each depolarizing stimulus, there is an exponential increase in blocked channels. During the interstimulus interval, there is a slow recovery from blockade. Where the time constant of recovery is less than one-fourth the interstimulus interval, the block acquired during depolarization is recovered during the interstimulus interval, with the result of no apparent "use dependence." As the interstimulus interval is reduced, though, use dependence can be observed. After a number of stimuli, a steady state condition will be achieved when the block acquired during the depolarization period is equal to that lost during the interstimulus interval. The symbols, b_i, indicate the level of block just prior to the depolarizing stimulus. The symbols, a_i, indicate the level of block immediately after the depolarizing period. At steady state, $a_n = a_{n+1}$ and $b_n = b_{n+1}$.

Let a_∞ be the equilibrium block associated with the depolarizing phase of the stimulus and b_∞ be the equilibrium block associated with the repolarizing phase of the stimulus protocol. For the nth stimulus in the pulse train, blockade immediately before depolarization (b_n) and immediately after depolarization (a_n) is described by

$$b_n = a_{n-1}e^{-t_r/\tau_r} + b_\infty(1 - e^{-t_r/\tau_r}) \tag{6}$$

$$a_n = b_n e^{-t_d/\tau_d} + a_\infty(1 - e^{-t_d/\tau_d}) \tag{7}$$

where

$$a_\infty = \left(1 + \frac{g_d l}{f_d kD}\right)^{-1}, \quad \tau_d = (f_d kD + g_d l)^{-1} \tag{8}$$

and

$$b_\infty = \left(1 + \frac{g_r l}{f_r kD}\right)^{-1}, \quad \tau_r = (f_r kD + g_r l)^{-1} \tag{9}$$

The blocking equations can be more conveniently written as

$$a_n = b_n e^{-t_d/\tau_d} + A \tag{10}$$

$$b_{n+1} = a_n e^{-t_r/\tau_r} + B \tag{11}$$

Substitution yields the two recurrence blockade equations

$$a_{n+1} = a_n e^{-\lambda} + Be^{-t_d/\tau_d} + A \tag{12}$$

$$b_{n+1} = b_n e^{-\lambda} + Ae^{-t_r/\tau_r} + B \tag{13}$$

where λ, the uptake rate constant, is a linear combination of the two reciprocal time constants

$$\lambda = t_d/\tau_d + t_r/\tau_r \tag{14}$$

and thus dependent on the various rate constants, stimulus parameters, and drug concentration.

For an initial fraction of blocked channels, b_0, the two recurrence equations can be solved to give the fraction of blocked channels associated with the nth stimulus

$$b_n = b_0 e^{-n\lambda} + \frac{(Ae^{-t_r/\tau_r} + B)}{1 - e^{-\lambda}}(1 - e^{-n\lambda}) \tag{15}$$

$$= b_{ss} + (b_0 - b_{ss})e^{-n\lambda} \tag{16}$$

and

$$a_n = a_0 e^{-n\lambda} + \frac{(Be^{-t_d/\tau_d} + A)}{1 - e^{-\lambda}}(1 - e^{-n\lambda}) \tag{17}$$

$$= a_{ss} + (a_0 - a_{ss})e^{-n\lambda} \tag{18}$$

The coefficients a_{ss} and b_{ss} represent the "quasi" equilibrium or "steady state" block acquired after many pulses. At steady state, when $a_n = a_{n+1}$ and $b_n = b_{n+1}$, blockade is expressed by

$$a_{ss} = \frac{a_\infty(1 - e^{-t_d/\tau_d}) + e^{-t_d/\tau_d}b_\infty(1 - e^{-t_r/\tau_r})}{1 - e^{-\lambda}} \tag{19}$$

$$b_{ss} = \frac{b_\infty(1 - e^{-t_r/\tau_r}) + e^{-t_r/\tau_r}a_\infty(1 - e^{-t_d/\tau_d})}{1 - e^{-\lambda}} \tag{20}$$

When recovery potentials are sufficiently negative such that $f_r = 0$, then $b_\infty = 0$. The steady state blockade is simplified to

$$a_{ss} = a_\infty \frac{1 - e^{-t_d/\tau_d}}{1 - e^{-\lambda}} \tag{21}$$

$$b_{ss} = a_\infty \frac{e^{-t_r/\tau_r}(1 - e^{-t_d/\tau_d})}{1 - e^{-\lambda}} \tag{22}$$

Fig. 3 illustrates how the "phasic" steady state values, a_{ss} and b_{ss}, vary as functions of stimulus pulse interval. Increases in stimulus interval ($t_r + t_d$) lead to lower values of steady state block, reflecting the increased recovery period. Furthermore, the difference between the values of steady state block preceding and following depolarization becomes more pronounced with increases in the recovery interval. As we have seen from the definition of λ, the uptake rate is linearly related to drug concentration. Thus, as the concentration is increased, the steady state value of block increases. The difference between steady state block associated with different concentrations increases with increasing stimulus interval, again due to the prolongation of the recovery period, as shown in Fig. 4.

Hydrophobic and hydrophilic Paths. For local anesthetics, Hille (2) suggested the existence of two diffusion paths between drug pool and
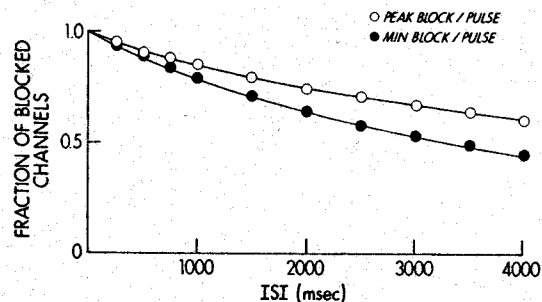
FIG. 3. *The effect of interstimulus interval on before (●) and after (○) stimulus blockade as interstimulus interval is varied*

Data points are based on constants derived from propafenone in ventricular muscle. At very high stimulus rates (*isi* < 500 msec), block is nearly complete with very little difference between the end stimulus interval blockade and the end depolarization interval blockade. As the interstimulus interval is increased, the cumulative use-dependent blockade is reduced, as is the difference between end stimulus interval and end depolarization blockade. This reflects loss of block during the additional recovery interval.

FIG. 4. *The effect of interstimulus interval and drug dose on end stimulus interval blockade*

Using rate constants derived from propafenone in ventricular muscle, use-dependent block at doses of 50 μM (O) and 5 μM (●) was computed using Equation 21.

the receptor-binding site: a hydrophobic or membrane path, and a hydrophilic or aqueous path. In general, charged agents are hydrophilic, so their receptor access is predominantly by the aqueous path, while neutral agents are hydrophobic, so their receptor access is by the membrane path. A tertiary amine partitioned into neutral, D^o, and cationic, D^+, forms would presumably interact with the channel via both diffusion paths with possibly path-dependent gating effects and rate constants.

With the Hodgkin-Huxley formalism of sodium channel gating (18), we define the guard and trap functions in terms of the inactivation gate, h, and the activation gate, m^3. Since open channels are required for aqueous path access (6) and also for unbinding (12), we have defined $f = m^3h$ and $g = m^3h$ for hydrophilic agents. Lipid-soluble agents appear to only require an open conformation m^3 process for binding (14) and can unblock at any time, so we define $f = m^3$ and $g = 1$ for hydrophobic agents.

With these definitions in mind, for pure hydrophilic agents, the binding process is characterized by

$$U + D^+ \underset{m^3hl^+}{\overset{m^3hk^+}{\rightleftharpoons}} B^+$$

where open channels are required for both binding and unbinding. For hydrophobic agents, the binding process is characterized by

$$U + D^o \underset{l^o}{\overset{m^3k^o}{\rightleftharpoons}} B^o$$

where the access path is now controlled in the binding direction by the m^3 gate conformation, but the unbinding path is uncontrolled.

For a tertiary amine, blockade is dependent on both paths where the relationship between external pH and drug pK determines the relative importance of either path. Furthermore, for tertiary agents there is proton exchange between charged blocked and uncharged blocked channels (7) which couples the hydrophobic and hydrophilic binding processes and is characterized by

$$
\begin{aligned}
U + D^o &\underset{l^o}{\overset{m^3k^o}{\rightleftharpoons}} \quad\;\; \begin{matrix} B^o \\ + \\ H^+ \end{matrix} \\
U + D^+ &\underset{m^3hl^+}{\overset{m^3hk^+}{\rightleftharpoons}} \begin{matrix} k_p \updownarrow l_p \\ B^+ \end{matrix}
\end{aligned}
$$

where k_p and l_p represent the protonation and deprotonation rates associated with blocked channels.

Derivation of the recursive equations for a mixed path follows the derivation for a single path, as illustrated above. The major result is that the single exponential characterization of blockade is now represented by the sum of several exponentials whose rates are dependent on the path specific guard and trap functions, binding and unbinding parameters, pH, pK of drug, proton exchange rates, and drug concentration.

RESULTS

Analysis procedure. The primary theoretical results from the analysis of drug binding to a periodically accessible binding site are summarized as follows. 1) The sequence of observed fractions of bound sites follows an exponential time course described by

$$a_n = a_{ss} + (a_0 - a_{ss})e^{-n\lambda}. \tag{23}$$

2) The uptake rate, λ, is linearly related to the stimulus interval, binding site access interval, and drug concentration

$$\lambda = (f_dkD + g_dl)t_d + (f_rkD + g_rl)t_r. \tag{24}$$

3) For sufficiently negative membrane potentials, the steady state fraction of bound sites, a_{ss}, is related directly to the equilibrium fraction of bound sites and inversely to a function of the uptake rate.

$$a_{ss} = a_\infty \frac{1 - e^{-t_d/\tau_d}}{1 - e^{-\lambda}} \tag{25}$$

These three relationships form both a basis for testing whether a periodically activated blockade process follows a sequence of bimolecular binding reactions and a method for estimating the apparent binding parameters, k and l. From measures of blockade acquired with pulse train stimulation, each of the above relationships can be tested. For instance, does the stimulus-to-stimulus measure of blockade follow a single exponential time course (evidence of a dominant single access path and first order binding)? For multiple stimulus rates, does the rate of blockade development, λ, vary linearly with stimulus interval and drug concentration? For multiple stimulus rates, does the steady state level of blockade vary linearly with $(1 - e^{-\lambda})^{-1}$?

The details of a procedure to estimate k and l depend on the assumed guarding and trapping functions. The simplest example is to consider a guarding function that is 1 during the access interval and 0 during the recovery interval. The simplest trapping function is to assume it to be 1 during the entire stimulus interval. For these functions, the uptake rate, λ, is described by

$$\lambda = (kD + l)t_d + lt_r. \tag{26}$$

Analysis of records of use-dependent blockade is carried out by first assessing the goodness of fit between observed blockade and predicted blockade based on a least-squares fit of Equation 23 to the data. For each stimulus rate, the parameters a_0, a_{ss}, and λ are estimated using a nonlinear least squares procedure (15). Assuming an access time of 1 msec, the recovery time, t_r, is approximated by the difference between the interstimulus interval and access time. From a regression of λ, estimated from the use-dependent uptake curves, against t_r, the slope and intercept are used to estimate k and l. The model is then verified by plotting observed steady state blockade, a_{ss}, against $(1 - e^{-\lambda})^{-1}$. The resulting curve should be linear and pass through the origin. In addition, the use-dependent blockade curve can be reconstructed with estimates of k, l, drug concentration, and the stimulus parameters t_d and t_r. From these values, a_{ss} is

computed from Equation 25 and λ is computed from Equation 24. The predicted use-dependent curve is then computed according to Equation 23.

Summarizing the procedure, for each uptake curve, values of λ and a_{ss} are estimated and the value of the stimulus interval, isi, is recorded. From a regression of λ on t_r, a slope and intercept are determined. From a regression of a_{ss} on $(1 - e^{-\lambda})^{-1}$ an additional slope and intercept are determined. If this intercept is not near zero, there may be significant resting block. From the resulting three parameters (two slopes and an intercept), three model parameters can be estimated. These will include the binding parameters, k and l. A third parameter that must occasionally be estimated is the fraction of unguarded receptors at the resting potential. (Some stimulus protocols do not use a sufficiently negative resting potential to drive f_r to zero. This results in a "resting block.") These values are used in Equations 23, 24, and 25 to compute expected values of channel blockade.

Examples. Investigating how well this simplified discrete blockade process describes phasic ion channel blockade, we selected several studies for analysis: studies of lidocaine blockade in skeletal muscle (7), studies of propafenone blockade in cardiac muscle (8), and studies of quinidine blockade in cardiac muscle (16). Each of these studies used repetitive stimulation to modify the fraction of blocked ion channels. For each study, we estimated a single apparent forward (k) and reverse (l) rate constant. With these parameters, we assessed the adequacy of the underlying bimolecular binding model by predicting the time course of use-dependent blockade with Equation 23 using the estimated k and l, while varying only the stimulus rate.

Use-dependent patterns of blockade followed a single exponential in each of three studies, suggesting one dominant uptake path, one dominant recovery path, and a dominant active blocking moiety. Therefore, we used the following bimolecular binding scheme for our analysis

$$U + D \overset{fk}{\underset{l}{\rightleftharpoons}} B$$
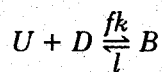
where f was assumed to be 1 during the access interval and 0 during the recovery interval.

Using 0.2 mM lidocaine at pH 6.0, Schwarz *et al.* (7) induced channel blockade at stimulus intervals of 3200, 1600, 800, 400, 200, and 100 msec. Inward sodium current was determined in skeletal muscle using voltage clamp procedures. We selected the three slow pulse rates for estimating the rate constants. A fourth curve was analyzed independently to test the predictive accuracy of Equation 26.

Associated with each pulse train was a different steady state fraction of blocked channels and a different time constant for achieving steady state block. Using Equation 23 to describe measured phasic blockade, the stimulus intervals of 3200, 1600, 800, and 400 yielded uptake rates, λ, of 0.112, 0.095, 0.0865, and 0.078, as determined by a nonlinear least squares fit. A regression of λ against stimulus interval using the uptake rates associated with three slower stimulus intervals (Fig. 5) yielded a slope of
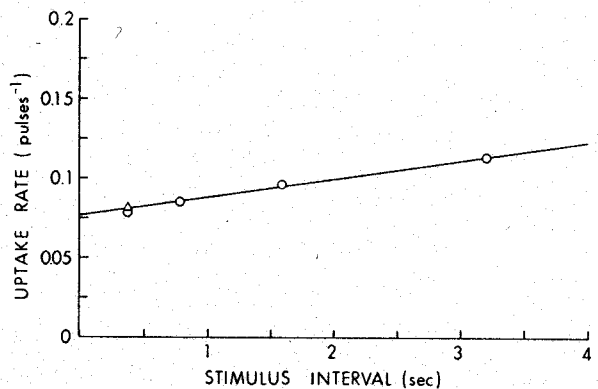
FIG. 5. *Relationship between uptake rate and stimulus interval*

According to the theoretical model, uptake rate should be linearly related to stimulus interval as described by Equation 14. Uptake rates estimated from the use-dependent curves of lidocaine at stimulus intervals of 3.2, 1.6, 0.8, and 0.4 sec are plotted against the recovery interval. The rates from the three slower stimulus rates were used to compute the displayed regression line. The $\triangle$ indicates the predicted uptake rate for 0.4-sec stimulation and compares favorably with the observed rate plotted immediately above it.
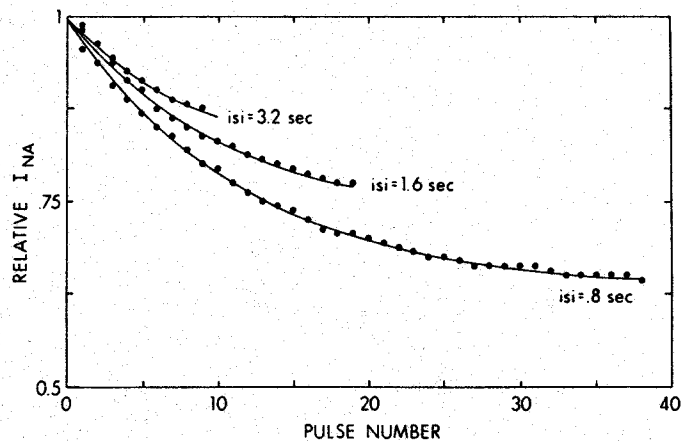

FIG. 6. *Observed and computed reduction in relative I_{Na} with 0.2 mM lidocaine*

For each stimulus rate, the aggregate exponential decay rate, λ, was estimated by least squares. From the resulting values of λ and their corresponding values of isi, forward (k) and reverse (l) rate constants were estimated from Equation 26. With these two constants fixed, relative I_{Na} for each stimulus was computed from Equations 23 and 25, with relative $I_{Na} = (1 - a_n)/(1 - a_0)$.

TABLE 1

Uptake rate and steady state block for propafenone

Stimulus interval	Uptake rate (λ)	Steady state block (a_{ss})
msec	*pulse*$^{-1}$	
1000	0.435	0.785
2000	0.517	0.646
5000	0.808	0.465

1.06×10^{-5} pulse^{-1} sec^{-1} and an intercept of 0.07790. Testing the generality of the linear relationship, we estimated a λ for a 400-msec interval of 0.081 (plotted as a $\triangle$ in Fig. 5). This value is close to the observed uptake rate at 400 msec of 0.078. Assuming an average channel open time of 1 msec resulted in estimates of $k = 3.90 \times 10^{2}$ M^{-1} msec^{-1} and $l = 1.06 \times 10^{-5}$ msec^{-1} for a
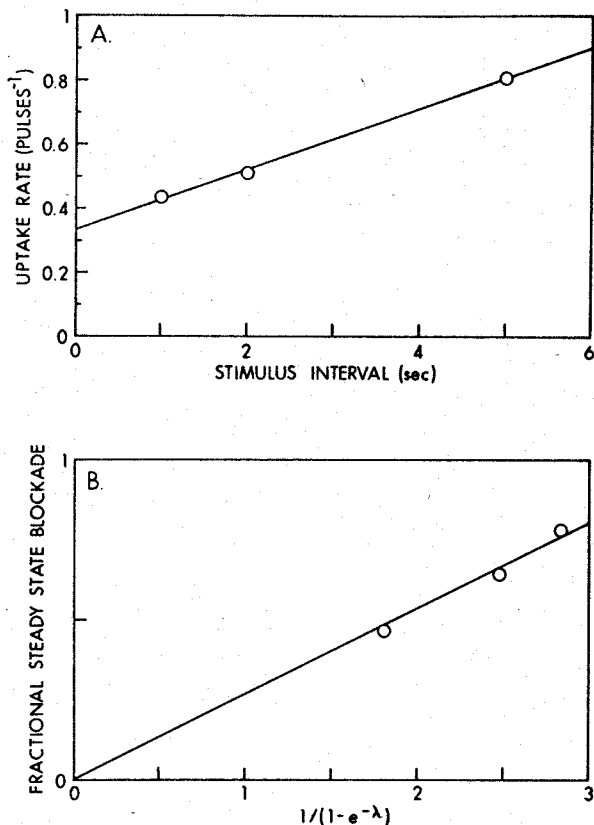
FIG. 7. *Relationship between uptake rate, steady state blockade, and stimulus interval*

Panel A illustrates the linear relationship between uptake rate and stimulus interval. Though there are only three data points, there is good agreement with the theoretically predicted linear relationship. Panel B illustrates the relationship between steady state blockade and $(1 - e^{-\lambda})^{-1}$. With values of uptake rate and steady state blockade determined by a least squares fit of the use-dependent uptake of propafenone, the plotted points are clearly in agreement with the theoretical prediction of a linear relationship with an intercept at the origin.

resting potential of −100 mV. Using these two rate constants and the stimulus intervals, Equation 23 was evaluated for 50 pulses ($n = 0, 1, 2 \ldots 49$). The resultant predicted values, along with experimentally observed values, are shown in Fig. 6. Since Schwarz *et al.* reported their data in terms of normalized I_{Na}, initial block was adjusted in order to optimize agreement between observed and predicted steady state block. Because the data were normalized, it was not possible to evaluate the steady state block relationship (Equation 25).

Kohlhardt and Seifert (8), in studies of the effect of propafenone on ventricular muscle, found variations in apparent receptor affinity at different stimulation rates, as measured by the maximum rate of rise of the action potential $\dot{V}_{max}$. Thus, we were interested in determining whether a constant affinity guarded receptor would produce such shifts in apparent affinities.

The results of fitting an exponential to the use-dependent curves are shown in Table 1. The relationship between uptake rate and stimulus interval is shown in panel A of Fig. 7, and a least squares fit of the line yields a slope of 9.5×10^{-5} msec^{-1} and an intercept of 0.34. A

further test of the underlying model is shown in panel B of Fig. 7. Here we have plotted the steady state block against $(1 - e^{-\lambda})^{-1}$. The theoretical relationship as defined by Equation 25 should be linear and pass through the origin. The observed relationship confirms the theoretical prediction.

Assuming a 1-msec average channel open time and using a concentration of 20 μM gives estimates of $k = 1.7 \times 10^4$ M^{-1} msec^{-1} and $l = 9.3 \times 10^{-5}$ msec^{-1} for a resting potential of −93 mV. Using these two apparent rate constants, Equations 23, 24, and 25 were used to estimate channel blockade at frequencies of 1/sec, 1/2 sec, and 1/5 sec, as shown in Fig. 8. The experimentally observed values of $\dot{V}_{max}$ are shown as filled circles (●), while predicted values are shown as empty circles (○).

Kohlhardt and Seifert (8) determined a dose-response relationship by stimulating at a rate of 2/sec, using the reduction in $\dot{V}_{max}$ associated with the first pulse to esti-
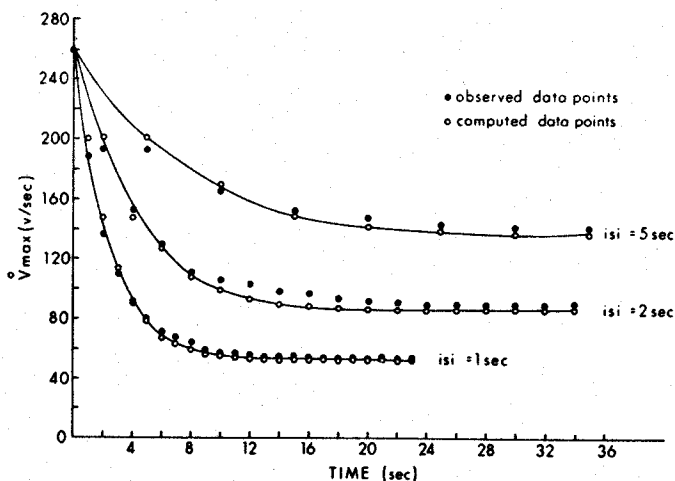

FIG. 8. *Observed and computed reduction in $\dot{V}_{max}$ with propafenone in ventricular muscle*

For each stimulus rate, the aggregate exponential decay rate, λ, was estimated by least squares. From the values of λ and the corresponding values of *isi*, a forward (k) and reverse (l) rate constant were estimated from Equation 26. With these two constants fixed, $\dot{V}_{max}$ reduction for each stimulus rate was computed from Equations 23 and 25, with $\dot{V}_{max} = \dot{V}_{max}(0)(1 - a_n)$. The reverse rate constants were computed from $l_r = le^{-V_{rest}F/RT}$, $l_d = le^{-V_{test}F/RT}$. The dose was 20 μM, as stated in Ref. 8.
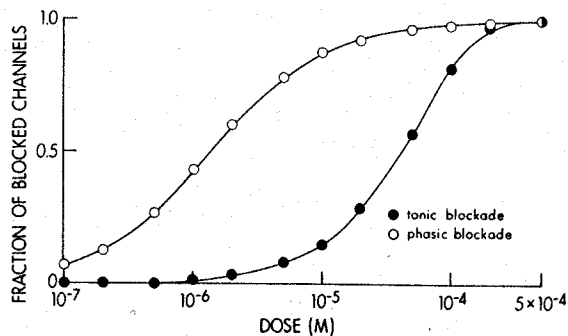

FIG. 9. *Dose-response curves of phasic (○) and tonic (●) block derived from Equations 23, 25, and 26, using rate constants estimated from propafenone uptake*

Tonic block measures blockade acquired prior to and during the first stimulus of a repetitive pulse train. Phasic block measures steady state blockade after many stimuli relative to tonic block.

TABLE 2

Observed and (predicted) uptake pulse constants (pulses) at isi = 0.5 sec

	pH 7.4	pH 6.9	pH 7.4
HCO_3^-	$6.2 \pm 1.5\ (3.8)$	$7.5 \pm 1.6\ (4.5)$	$6.3 \pm 1.4\ (4.2)$
CO_2	$5.8 \pm 1.5\ (7.1)$	$5.8 \pm 0.2\ (5.0)$	$5.9 \pm 0.6\ (7.7)$

mate tonic blockade and using the difference in $\dot{V}_{max}$ associated with steady state blockade and the first pulse blockade to estimate phasic blockade. Simulating this protocol, we computed blockade as a function of concentration using Equations 23, 24, and 25 at a stimulus rate of 2/sec, using the two rate constants estimated above. Fig. 9 shows the resulting dose-response curves for tonic and phasic block. The half-response concentration for phasic block (open circles) was 2.5 μM, while the half-response concentration for tonic block (filled circles) was 50 μM. These values are considerably larger than the equilibrium K_d, based on the estimated forward and reverse rate coefficients ("true" $K_d = 0.136$ nM with $V_{mem} = 0$ mV). The differences are due to the relatively long block recovery period (499 msec), in contrast to an uptake period of 1 msec. By increasing the frequency of stimulation, the phasic blockade K_d decreases in concert with a decreasing recovery period. In the limit as the access time becomes continuous, phasic K_d will approach the "true" K_d. In other words, both exponentials in Equation 25 will be essentially zero, resulting in the steady state block being equal to the equilibrium block.

Grant *et al.* (16), in studies of pH effects on quinidine blockade in guinea pig ventricular myocardium, observed both blockade onset and recovery at stimulus intervals of 500 and 1000 msec. Blockade onset was observed during a 20-sec train of stimuli at one of the two stimulus intervals. Recovery from blockade was assessed by inserting test pulses between pulse trains used to "load" the channels with blocking agent. Data from Table 2 in Grant *et al.* (16) was used to estimate forward and reverse rates.

For stimulus intervals of 500 and 1000 msec, the action potential duration was observed to be approximately 200 msec. Though not clearly established, we assume for illustrative purposes that quinidine access is primarily through the hydrophobic path, characterized by a mean receptor access time, t_d, of approximately 200 msec. Using Equation 26 as the definition of λ, the parameter, kDt_d, was estimated from the 1000-msec data in Grant's Table 2, using

$$kDt_d = \left(\lambda_{1000} - \frac{0.8}{\tau_r} \right) \quad (27)$$

where $\lambda_{1000} = \tau^{-1}$ (inverse onset pulse constant), and τ_r is the average observed recovery time constant. Uptake pulse rates for stimulus intervals of 500 msec were estimated by

$$\lambda_{500} = kDt_d + \frac{0.3}{\tau_r} \quad (28)$$

and the corresponding uptake pulse constants, τ_u, were computed from λ_{500}^{-1}. These values are summarized in Table 2 and are mostly within the variations associated

with the original observed constants described in Grant's Table 2 and Fig. 4. Grant's results are reported as a mean $\pm$ 1 SE.

DISCUSSION

Courtney *et al.* (17), in an elegant analysis of ion channel blockade, first proposed characterizing phasic channel blockade associated with each stimulus as a two-step process: 1) a discrete step of drug incorporation during the interval of depolarizing potential followed by 2) continuous drug release during the interval of resting potential. The discrete step of drug incorporation, though, is the result of a binding process taking place during the interval when the receptor is accessible. Single channel observations suggest receptor accessibility is pulselike in nature (9, 10). Thus, in order to simplify the channel-gating model, we assumed that all binding sites operate in a synchronized fashion where they become accessible simultaneously and remain accessible for a fixed period of time. For illustrative purposes, we assumed that the interval between the end of the accessible interval and membrane repolarization is negligible. We then assumed first order binding during the accessible interval. This is a generalization of Courtney's approach, in that continuous blockade occurs during both uptake and recovery periods. The resulting quantitative framework describes channel blockade with fewer rate constants than the modulated receptor hypothesis and does not require modified inactivation gate kinetics in drug-complexed channels. Furthermore, it provides a theoretical basis for observations of exponential uptake of blocking agents (8, 16, 18) and a linear relationship between uptake rate and drug concentration (18).

We have made several simplifying assumptions that appear justified based on agreement between experimentally observed blockade and that predicted by theory. We have assumed a constant receptor access time equal to the mean receptor access time (see "Appendix") and have assumed state transitions to be fast. Also, we have assumed that when the depolarizing stimulus duration exceeds the mean access time, the interval between the time the receptor becomes inaccessible and repolarization can be ignored. Perhaps the weakest assumption is that all three drugs utilize a single diffusion path, although almost certainly both neutral and charged moieties and their respective diffusion paths participate in the blockade process. The excellent fits of the data for lidocaine and propafenone suggest that the hydrophilic path may be the dominant path for drug ingress (forward velocity proportional to m^3hk), while the hydrophobic path may be the dominant path for drug egress (reverse velocity not gate dependent). Should this be the case, the estimated unbinding rate, l, reflects both unbinding and deprotonation of a charged blocking agent. For quinidine, we assumed hydrophobic access with an access time determined by the action potential duration. These assumptions may change as better data become available.

The theoretical properties of periodically activated binding sites as described in Equations 23, 24, and 25 provide tools for testing the adequacy of a proposed binding process. Deviations from a monoexponential

time course, as specified by Equation 23, suggest that there may be multiple diffusion paths with perhaps different guard and trap mechanisms. Deviations from a linear relationship between uptake rate, drug concentration, and stimulus interval suggest that guarding and trapping may not be a pulselike process, i.e., transitions between guard and trap states may not be fast enough to be neglected.

The unguarded interval is used to compute the recovery interval ($t_r = isi - t_d$). Thus, if the incorrect unguarded interval is assumed, the intercept of the λ *versus* t_r line may be negative, implying a negative binding rate. A larger value of t_d reduces t_r, thereby shifting the line to the left. Finally, deviations from a linear relationship between steady state blockade and $(1 - e^{-\lambda})^{-1}$ may indicate additional problems with the uptake rate constant, λ, or the assumed guard or trap functions, or that there is a significant amount of resting block at the recovery potential.

The blockade model we have presented was developed for a single diffusion path. We do not imply that all blocking agents can be characterized by this same strategy. Our approach is not meant as a rigid universal description of blockade but more as a "generic" description that can be easily extended to fit the detailed experimental protocol, drug characteristics, active diffusion paths, and gate trapping. Thus, extension to >2-phase stimulus pulse trains is necessary for certain protocols where these features are significant determinants of channel blockade.

Extension to two diffusion paths is probably necessary for drugs with a pK near physiologic pH. For conditions of constant pH and where one moiety dominates, this extension appears unnecessary, as shown by the lidocaine, quinidine, and propafenone data presented. When significant fractions of both moieties are present, the two-path model must be used. The mathematical description of two-moiety blockade will display a multiexponential pattern of use dependence, in contrast to the monoexponential pattern exhibited by a single agent. When the two moieties are neutral and charged derivatives of a parent blocking agent, the mathematical description must further contain the proton exchange process that couples a charged blocked channel with a neutral blocked channel. For this multimoiety process, a more complex experimental protocol is required in order to estimate the rate constants associated with each moiety.

For a single set of binding and unbinding rates, it is only necessary to vary, as part of the experimental protocol, either stimulus rate or drug concentration in order to generate the required variations in uptake rate sufficient for parameter estimation. For two moieties, the differential contribution of each agent to total blockade must be varied in order to estimate the associated rate constants. This is probably best achieved by varying the pH, thereby varying the ratio of D^+ to D^0. Combinations of variations in pH, stimulus rate, and drug concentration will produce variations in uptake rate that are theoretically adequate for isolating the binding parameters.

Extension of the analytic description of ion channel blockade to multiple drugs or multiple diffusion paths follows the procedure we used for a single-path two-phase stimulus protocol. Though algebraically tedious, the extension is straightforward.

We showed above that as the receptor access period increases, the apparent k_d for a transiently accessible binding site becomes equivalent to that determined for continuously accessible receptors. This equivalence will possibly aid in relating the results of ligand-binding studies to results from electrophysiologic studies. Recently, Bean (19) has shown that for the calcium channel antagonist, nitrendipine, the apparent k_d determined from measures of Ca^{2+} current under conditions of long depolarizations are in agreement with results obtained from equilibrium-binding studies with membrane fragments. From Equation 1 we would expect the k_d to be a function of both the guard and trap functions as

$$k_d = \frac{gl}{fk} \tag{29}$$

Since nitrendipine is lipophilic, one would expect g to be 1 and f to be the fraction of activated calcium channels (similar to the m^3 function for sodium channels). Thus, under the depolarization conditions used by Bean (−10 mV), f would be near 1, and indeed the electrophysiologic determination should agree with the ligand-binding studies. For the more polarizing potential (−80 mV), the apparent k_d was significantly larger as predicted by our theory, since fewer channels would have had unguarded binding sites.

This model of transiently accessible receptor binding provides a simple and unifying conceptual base on which ion channel blockade can be explained. It is hoped that parameters estimated by the procedures described here will aid in characterizing the relationship between structure and function of pharmacologic ion channel-blocking agents. Furthermore, this theoretical scheme may be applicable when describing the behavior of any bimolecular process that is periodically activated. Thus it may be useful in characterizing receptor processes outside the ion channel blockade arena.

APPENDIX

Channel blockade with stochastic receptor access time

For illustrative purposes, assume channel opening is synonymous with receptor accessibility. Assuming that channel open and close events are probabilistic Poisson events, the probability density of a channel closing at time t, given it was open at time 0, is:

$$p(t) = \lambda e^{-\lambda t} \tag{30}$$

where λ is the closing event rate. The mean channel open time is $1/\lambda$. During the channel open period, drug binding to the receptor follows an exponential time course

$$b(t) = b(\infty) + (b(0) - b(\infty))e^{-(kD+l)t} \qquad (31)$$

The expected block for an ensemble of channels is

$$\langle b \rangle = \int_0^\infty \lambda b(t)e^{-\lambda t}\, dt \qquad (32)$$

$$= b(\infty) + (b(0) - b(\infty))\frac{\lambda}{\lambda + kD + l} \qquad (33)$$

For a constant channel open time of $1/\lambda$, the blockade based on Equation 31 would be

$$b = b(\infty) + (b(0) - b(\infty))e^{-(kD+l)/\lambda} \qquad (34)$$

To a first order approximation, the exponential can be represented by the first two terms of its series expansion, such that

$$e^{-(kD+l)/\lambda} = \frac{1}{e^{(kD+l)/\lambda}} \approx \frac{1}{1 + \dfrac{kD+l}{\lambda}} = \frac{\lambda}{\lambda + kD + l} \qquad (35)$$

Replacing the exponential in Equation 34 with its series approximation (Equation 35) yields Equation 33, the ensemble blockade acquired during a stochastic channel open time. Thus, using a constant channel open time equal to the mean channel open time for estimating channel blockade closely approximates the correct fraction of blocked channels.

When the depolarization time is long (>2–3 msec) in contrast to the mean channel open time ($\approx$1 msec), an additional assumption is required. If the channel opens immediately following depolarization and closes prior to repolarization, a period when the membrane is depolarized yet the channel is closed will exist. We currently ignore this period, since for the voltage clamp stimulus protocols studied, this period is short relative to the repolarization interval.

REFERENCES

1. Starmer, C. F., A. O. Grant, and H. C. Strauss. Mechanisms of use-dependent block of sodium channels in excitable membranes by local anesthetics. *Biophys. J.* 46:15–27 (1984).
2. Hille, B. Local anesthetics: hydrophilic and hydrophobic pathways for the drug-receptor reaction. *J. Gen. Physiol.* 69:497–515 (1977).
3. Hondeghem, L. M., and B. G. Katzung. Time and voltage-dependent interactions of antiarrhythmic drugs with cardiac sodium channels. *Biochim. Biophys. Acta* 472:373–398 (1977).
4. Courtney, K. R. Mechanisms of frequency-dependent inhibition of sodium currents in frog myelinated nerve by the lidocaine derivative GEA968. *J. Pharmacol. Exp. Ther.* 195:225–236 (1975).
5. Bean, B. P., C. M. Cohen, and R. W. Tsien. Lidocaine block of cardiac sodium channels. *J. Gen. Physiol.* 81:613–642 (1983).
6. Strichartz, G. R. The inhibition of sodium currents in myelinated nerve by quaternary derivatives of lidocaine. *J. Gen. Physiol.* 62:37–57 (1973).
7. Schwarz, W., P. T. Palade, and B. Hille. Local anesthetics: effect of pH on use-dependent block of sodium channels in frog muscle. *Biophys. J.* 20:343–368 (1977).
8. Kohlhardt, M., and C. Seifert. Tonic and phasic I_{Na} blockade by antiarrhythmics. *Pfluegers Arch. Eur. J. Physiol.* 396:199–209 (1983).
9. Grant, A. O., C. F. Starmer, and H. C. Strauss, Unitary sodium channels in isolated cardiac myocytes of rabbit. *Circ. Res.* 53:823–829 (1983).
10. Cachelin, A. B., J. E. DePeyer, S. Kokubun, and H. Reuter. Sodium channels in cultured cardiac cells. *J. Physiol. (Lond.)* 340:389–401 (1983).
11. Yeh, J. Z. Dynamics of 9-aminoacridine block of sodium channels in squid axons. *J. Gen. Physiol.* 73:1–21 (1979).
12. Yeh, J. Z., and J. Tanguy. The Na activation gate modulates slow recovery from use-dependent block by local anesthetics in squid giant axons. *Biophys. J.* 47:686–694 (1985).
13. Hodgkin, A. L., and A. F. Huxley. A quantitative description of membrane current and its application to conduction and excitation in nerve. *J. Physiol. (Lond.)* 117:500–544 (1952).
14. Weld, F. M., J. Coromilas, J. N. Rottman, and J. T. Bigger. Mechanisms of quinidine-induced depression of maximum upstroke velocity in ovine cardiac Purkinje fibers. *Circ. Res.* 50:369–376 (1982).
15. Marquardt, D. W. An algorithm for least-squares estimation of nonlinear parameters. *J. Soc. Ind. Appl. Math.* 11:431–441 (1963).
16. Grant, A. O., J. L. Trantham, K. K. Brown, and H. C. Strauss. pH-dependent effects of quinidine on the kinetics of dV/dt_{max} in guinea pig ventricular myocardium. *Circ. Res.* 50:210–217 (1982).
17. Courtney, K. R., J. J. Kendig, and E. N. Cohen. The rates of interaction of local anesthetics with sodium channels in nerve. *J. Pharmacol. Exp. Ther.* 207:594–604 (1978).
18. Gintant, G. A., Hoffman, B. F., and R. E. Naylor. The influence of the molecular form of local anesthetic-type antiarrhythmic agents on reduction of the maximal upstroke velocity of canine cardiac Purkinje fibers. *Circ. Res.* 52:735–746 (1983).
19. Bean, B. P. Nitrendipine block of cardiac calcium channels: high affinity binding to the inactivated state. *Proc. Natl. Acad. Sci. USA* 81:6388–6392 (1984).

Send reprint requests to: Dr. C. Frank Starmer, Departments of Medicine and Computer Science, Duke University Medical Center, Durham, NC 27710.